Aerosol and Air Quality Research

ORIGINAL RESEARCH
https://doi.org/10.4209/aaqr.240093

# Ultrafine Particles Monitoring in Paris: From Total Number Concentrations to Size Distributions Measurements

**Grégory Abbou[1*], Véronique Ghersi[1], François Gaie-Levrel[1], Anne Kauffmann[1], Mikael Reynaud[1], Christophe Debert[1], Philippe Quénel[1,2], Alexia Baudic[1*]**

[1] Airparif, The Air Quality Observatory within the Greater Paris Area, 75004 Paris, France
[2] University of Rennes, EHESP, Inserm, IRSET UMR S 1085, 35000 Rennes, France

## ABSTRACT

Due to their small size and ability to penetrate deeply into the respiratory system, ultrafine particles (UFP) pose a significant health risk. Their concentrations and sources are not consistently monitored and regulated in urban areas, including Paris. This study aims at presenting an overview of UFP measurements carried out in Paris from October 2019 to December 2022 using a mobility particle size spectrometer (MPSS). An averaged particle number concentration (PNC) of 8,100 ± 4,800 # $cm^{-3}$ was recorded between 8 and 100 nm on the analysis period, which was consistent with UFP concentrations usually observed in urban background conditions (< $10^4$ # $cm^{-3}$). The maximum PNC often exceeded World Health Organization (WHO) indicative values (10,000 # $cm^{-3}$ and 20,000 # $cm^{-3}$ daily and hourly averages respectively), thus emphasizing the need for ongoing UFP monitoring in Paris city. At the annual scale, averaged UFP concentrations were lower in 2020 (6,600 ± 3,900 # $cm^{-3}$) compared to 2021 and 2022 (8,100 ± 4,600 # $cm^{-3}$ and 8,700 ± 4,700 # $cm^{-3}$, respectively). This variability is depending on meteorological conditions and pollutant emissions, particularly during the first COVID-19 lockdown phase. UFP cycles can be attributed to anthropogenic emissions, mainly from road-traffic, with hourly maximum concentrations correlated with black carbon (BC, $r$ = 0.50 with $p \leq 0.05$). A correlation analysis with other pollutants also allowed to confirm road-traffic as a major UFP source in Paris due to high UFP associations with nitrogen dioxide ($NO_2$, $r$ = 0.58 with $p \leq 0.05$) and organic matter (OM, $r$ = 0.53 with $p \leq 0.05$). Concerning particle number size distribution (PNSD) measurements, a predominant particle mode between 20 and 30 nm (Aitken mode) was observed and linked to vehicular emissions. Finally, this study is worthwhile to support policymakers and to supply future epidemiological studies to better assess UFP health impacts with the ultimate aim of defining regulation thresholds.

**Keywords:** UFP, Urban air quality, MPSS, Number size distribution, Paris city

**OPEN ACCESS**

**Received:** April 3, 2024
**Revised:** September 23, 2024
**Accepted:** October 12, 2024

* **Corresponding Authors:**
Grégory Abbou
gregory.abbou@airparif.fr
Alexia Baudic
alexia.baudic@airparif.fr

**Publisher:**
Taiwan Association for Aerosol Research
**ISSN:** 1680-8584 print
**ISSN:** 2071-1409 online



## 1 INTRODUCTION

Ultrafine particles (UFP) constitute a research subject of growing interest, both in the deployment and application of new technologies dedicated to their measurements in specific contexts as well as in the knowledge of this emerging pollutant in atmospheric sciences. Particular attention is being paid to their sources, variabilities, but also to the processes governing their formation and aging in the atmosphere (Cassee *et al.*, 2019; Knibbs *et al.*, 2011; Rivas *et al.*, 2021; Trechera *et al.*, 2023). UFP are defined by the CEN/TC 264/WG 32 standard as aerosols with a diameter of 0.1 µm ($D_p \leq$ 100 nm) or less. These particles have the particularity of being difficult to qualify by gravimetric measurements, since they contribute very little to overall particle mass loading, notably for $PM_{10}$ and $PM_{2.5}$ monitored under European and national regulations (Kwon *et al.*, 2020). In urban areas, UFP contribute to more than 80% of total particle number concentrations (Dall'Osto *et al.*, 2013; Gani *et al.*, 2020) and may originate from a wide range of primary anthropogenic sources, mainly

related to combustion processes and gas-to-particles conversions (Gani *et al.*, 2020; Jimenez *et al.*, 2009; Setyan *et al.*, 2014; Xiao *et al.*, 2015; Zhang *et al.*, 2007). Due to their small size and large specific surface area, they can penetrate deep into the respiratory system, cross the alveolar-capillary barrier, reach sensitive organs and adsorb greater quantities of pollutants that can generate oxidative stress (Oberdörster *et al.*, 2005; Terzano *et al.*, 2010; Maher *et al.*, 2016; Schraufnagel *et al.*, 2019; Kwon *et al.*, 2020). Although many publications prove the existence of any relationships between short-term exposure to UFP and the occurrence of health impacts on the population (where causality currently seems to be accepted), existing literature suggests, however, that there is a lack of available scientific data to conclude on their potential long-term effects on the human body.

Several long-term datasets on aerosol particle number concentrations (PNC) and number size distributions (PNSD) were already obtained using stationary or mobile measurement sites in different cities (Hussein *et al.*, 2004; Charron and Harrison, 2003; Casquero-Vera *et al.*, 2021; Hopke *et al.*, 2022; Thén and Salma, 2022). More recently, a European study has published first results on UFP and PNSD collected in twenty-seven air quality monitoring sites from 2017 to 2019 (Trechera *et al.*, 2023). It is important to note that Paris (France) has not been included in this study due to the non-availability of data on this time period. However, it is worthwhile performing an unpublished comparable analysis for this city, as Paris is of a great interest for epidemiological studies due to its large amount of heath data and its high population density which provides a unique statistical power.

In that way, the present study should allow feeding into these health studies, which are partly based on the World Health Organization (WHO) recommendations. WHO recently proposed informative values to which UFP ambient concentrations can be compared in order to assess their dangerous nature and thus, guide decisions on priorities for controlling UFP sources (WHO, 2021). In accordance with the revision of the current ambient air quality directives (2008/50/EC and 2004/107/EC), the monitoring of total particle number concentrations (PNC) for particles in a diameter range from 10 nm to a few μm is highly recommended (European Parliament, 2022). When PNC are evaluated and compared to indicative values, it is of a great interest that policymakers can propose effective abatement strategies improving air quality and consequently, the knowledge of their main emitting sources is crucial. Nevertheless, only measuring total PNC does not meet such expectations. Only the use of a MPSS (Mobility Particle Size Spectrometer) can provide a more detailed documentation of submicron particle number levels and characterization of specific emission sources and/or formation processes.

In that context, this paper presents UFP measurements performed at a Paris urban background station using a MPSS. The objectives of this study were to (1) document the UFP concentrations, (2) describe their temporal variabilities, (3) provide a primary identification of UFP sources through a correlation study including particulate and gaseous pollutants, supplemented by an analysis of PNSD profiles, and (4) compare the measured concentrations to those observed in several world cities.

## 2 METHODS

### 2.1 Sampling Site and Measurement Period

The sampling site involved in this work is an urban background station located in the centre of Paris (48°51′44′′N–2°20′41′′E) in the Nelson Mandela garden nearly to the Forum des Halles mall (Fig. 1) in a much-used pedestrian environment both on weekdays and weekends. Apart from direct emission sources, this station is representative of average public exposure to air pollution levels in the Parisian conurbation. Considered as a reference site for the monitoring of various gaseous pollutants ($NO_x$, $O_3$, $CO/CO_2/CH_4$, $NH_3$) and physico-chemical parameters of interest in terms of aerosol health impacts (including $PM_{2.5}/PM_{10}$ mass concentrations, particulate matter in terms of number, size, chemical composition, precursor gases, oxidative potential), this station is considered as a supersite, in line with the WHO and European Parliament's recommendations.

The measurement period included a full three years (2020, 2021, and 2022) from October 15$^{th}$, 2019 up to December 31$^{st}$, 2022. It is important to note that 2020 was particularly marked by the

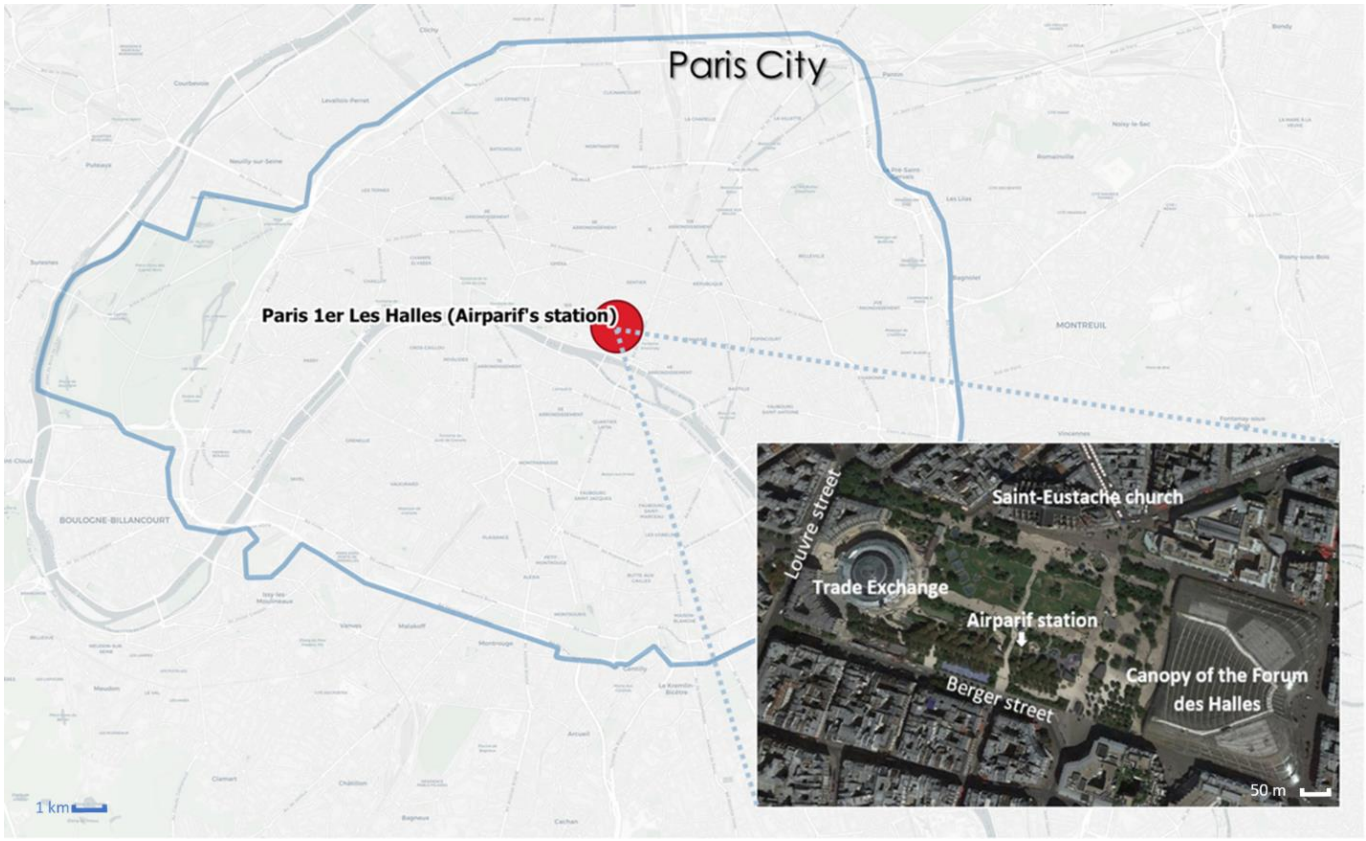


**Fig. 1.** Location of the Airparif's supersite in Paris-City, with a zoom at the neighborhood scale (right panel). (Sources: Carto Positron, Google Earth).

COVID-19 pandemic for which policy responses (public health measures, lockdowns, …) adopted worldwide were also implemented in France to limit the spread of the virus. They led to a significant reduction in economic activities and mobility, particularly in the transport sector (e.g., roads, civil aviation, railways). Such temporary restrictions have continued to take place through the year 2021. A gradual return to a pre-pandemic situation was noticeable in 2022.

## 2.2 Instrumentation

Ultrafine particles measurements were carried out using an electrical mobility spectrometer called MPSS in this paper (U-SMPS; PALAS GmbH, Karlsruhe, Germany) to monitor submicron PNSD. The U-SMPS includes a bipolar X-ray neutralizer (model 1297; PALAS GmbH), an electrostatic classifier (DEMC, models 1000 and 2000; PALAS GmbH) and a condensation nucleus counter (CNC, ENVI-CPC, model 100; Palas GmbH). The CNC was calibrated once a year and the X-ray source was changed every 8,000 hours in accordance with the CEN/TS 16976:2016 technical specification. Recommendations for MPSS measurements from 10 to 800 nm were also followed in this study (CEN/TS 17434:2020). Based on Wiedensohler *et al.* (2012), ACTRIS (2021) recommendations for the outdoor measurement of both UFP-PNSD and PNC are close to the CEN standards by allowing measurements below 10 nm if required. Such recommendations (Wiedensohler *et al.*, 2012, 2018) were followed concerning the operation, calibration and measurement uncertainties of the involved MPSS. For this study, the MPSS size range in terms of electrical mobility diameter ($d_{me}$) was covering 108 particle size classes ranging from 8 to 400 nm.

In parallel, black carbon (BC) concentrations were measured using an aethalometer (model AE33; Magee Scientific, Berkeley, California, USA) which allowed the identification of fossil-fuel ($BC_{ff}$) and biomass burning ($BC_{wb}$) fractions. The real-time chemical composition measurements of submicronic aerosols were provided by a quadrupole aerosol mass spectrometer (Q-ACSM; Aerodyne Research, Inc., Billerica, Massachusetts, USA). Although there are no regulations and

normative references for these two instruments, the quality assurance and control measures have been achieved in accordance with manufacturers' recommendations.

$PM_{10}$ and $PM_{2.5}$ mass concentrations were also monitored using an optical spectrometer (model FIDAS 200; Palas GmbH, Karlsruhe, Germany). Carbon monoxide/dioxide (CO, $CO_2$), methane ($CH_4$), and ammonia ($NH_3$) were measured by Cavity Ring-Down Spectroscopy (CRDS, models G2401 and G2103, Picarro). Ozone ($O_3$) was monitored by ultra-violet photometry (models O3-42M and O3-42e, ENVEA), while nitrogen monoxide and dioxide (NO, $NO_2$) were measured by a chemiluminescence analyzer (model 42i; Thermo Fisher Scientific, Waltham, Massachusetts, USA). The informations related to the quality assurance and control measures are presented in Table S1 for PM and Table S2 for gases, respectively.

## 2.3 Data Processing and Treatment

MPSS data were recorded with a 5-min time resolution and stored in a PostgreSQL database. Data processing and analyses were carried out using the R statistical software (v.4.1.2) and more precisely with the MyPUF package which is an open-source R library under a GNU license exclusively developed by Airparif. These were performed for averaged hourly PNC (in particles $cm^{-3}$, i.e., # $cm^{-3}$) from 8 to 400 nm ($N_{TOT}$: $N_{8\text{-}400}$), UFP size range ($N_{UFP}$: $N_{8\text{-}100}$) and for the nucleation ($N_{nuc}$: $N_{8\text{-}20}$), Aitken ($N_{Ait}$: $N_{20\text{-}100}$) and accumulation ($N_{acc}$: $N_{100\text{-}400}$) modes (ANSES, 2019; Kulmala *et al.*, 2004; Setyan *et al.*, 2014; Ling *et al.*, 2019; Chen *et al.*, 2022). The graphical visualization of UFP number concentrations time series at monthly, weekly and daily scales was made using the R Openair package (Carslaw and Ropkins, 2012). Calculations of smoothed curves from daily UFP measurements were performed using the stat_smooth function included in the R ggplot2 package. The R corrplot function was used for the correlations between $N_{UFP}$, $N_{nuc}$, $N_{Ait}$, $N_{acc}$, and other pollutants. The correlation coefficients were calculated with a *p*-value of 0.05, indicating that a probability of the observed results having occurred by chance is 5%. With a *p*-value $\leq 0.05$, results are typically considered significant, leading to the rejection of the null hypothesis $H_0$. The uncertainties shown for PNSD statistical diameters were obtained from laboratory tests on the reproducibility of four U-SMPS calculated according to ISO 5725-2 (1994).

Over the study period, more than 90% of data were available for processing and analysis—the missing data covering periods from April 19$^{th}$ to June 8$^{th}$, 2021 and from December 14$^{th}$, 2021 to January 24$^{th}$, 2022 were due to technical issues and calibration phases. All dates and hours referred in this article are in UTC (Coordinated Universal Time).

## 2.4 Dispersion Normalization Using Meteorological Data

To ensure a comparison of annual pollution concentrations by eliminating meteorological constraints, the "dispersion normalization" method (Chen *et al.*, 2022; Gani *et al.*, 2020; Sujatha *et al.*, 2016; Yang *et al.*, 2019) has been used. Designed to reduce the influence of atmospheric dispersion, this method aims to determine a ventilation coefficient ($VC_i$) for each i measurement, calculated as the product of boundary layer height (BLH, in meter) and wind speed (WS, in m $s^{-1}$):

$$VC_i = BLH_i \times WS_i \quad (1)$$

UFP number concentrations ($N_{UFPi}$) were therefore normalized as $N_{UFPnorm,i}$ to the average VC ($\overline{vc}$) calculated over the whole analysis period as:

$$N_{UFPnorm,i} = N_{UFPi} \times VC_{norm,i} \quad (2)$$

$$\text{with } VC_{norm,i} = VC_i / \overline{vc} \quad (3)$$

In this study, WS were recorded at the Paris-Montsouris weather station operated by the French national meteorological service Météo-France, while BLH were obtained from the Mesoscale Meteorological Mode version 5 (MM5) meteorological model (Dudhia and Bresch, 2002) using the geographic coordinates of the monitoring station. Both parameters were obtained at a 1-h time resolution.

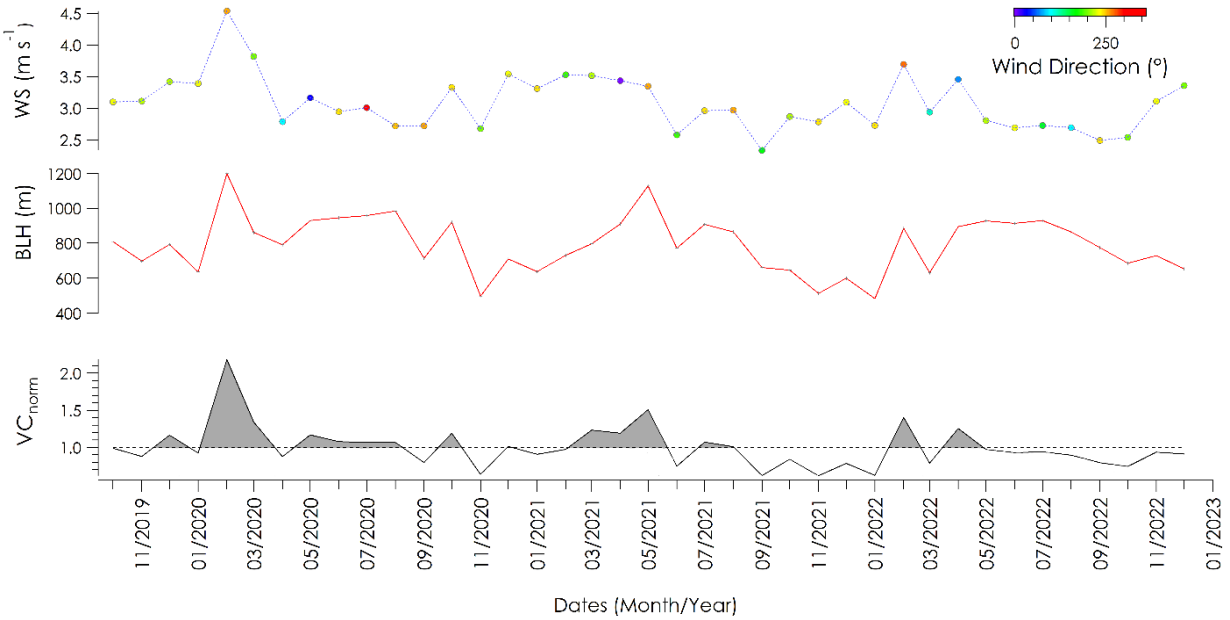


**Fig. 2.** Monthly timeseries of wind speed (WS) and wind direction (color scale), boundary layer height (BLH) and normalized ventilation coefficient ($VC_{norm}$, shaded areas corresponding to periods with $VC_{norm} > 1$) in Paris over the studied period.

# 3 RESULTS AND DISCUSSION

## 3.1 Overview of the Meteorological Parameters

Paris experimented a wide range of meteorological conditions with seasonal and diurnal variations in terms of ambient temperature, WS and BLH. Their seasonal and temporal evolutions are shown in Fig. S1. Fig. 2 shows the monthly variation of averaged WS and wind directions (color scale), BLH and $VC_{norm}$ over the study period. The average WS was around 3.1 m $s^{-1}$ ± 0.1 m $s^{-1}$ and remained within the same order of magnitude in 2020, 2021, and 2022 (3.2 m $s^{-1}$, 3.1 m $s^{-1}$, and 2.9 m $s^{-1}$, respectively). Maximum WS were reached in February 2020 (up to 4.5 m $s^{-1}$ on monthly average). This situation was also observed in terms of BLH with an altitude of 1,200 m. This results in a high $VC_{norm}$ coefficient (> 2), illustrating that February 2020 was particularly favorable to pollution dispersion.

It also should be noted that meteorological conditions were more dispersive in 2020 than in 2021 and 2022 (averaged $VC_{norm}$: 1.1 *versus* 0.96 and 0.93, respectively). The periods from February to March 2020, March to May 2021, and February and March 2022 (with the highest $VC_{norm}$ values) mainly occurred under the influence of southwesterly winds, which are characteristic of a disturbed oceanic flow associated with favorable pollution dispersion conditions (wind, rain and generally high BLH). Conversely, November 2020 and the second half of years 2021 and 2022 were poorly dispersive periods, i.e., represented by $VC_{norm}$ values less than 1.

## 3.2 Size-dependant Particle Number Concentrations

Table 1 presents averaged PNC for $N_{UFP}$ (8–100 nm) and $N_{TOT}$ (8–400 nm) and associated standard deviations measured at the Paris-Les Halles station for 2020, 2021, and 2022 years. Global hourly averages of 8,082 ± 4,772 # $cm^{-3}$ and 9,021 ± 5,145 # $cm^{-3}$ were calculated during the study period for $N_{UFP}$ and $N_{TOT}$, respectively. Such concentrations are in accordance with UFP concentrations measured in urban background situations (e.g., < 10,000 # $cm^{-3}$), as suggested by Cassee *et al.* (2019).

The relative percentage of $N_{UFP}$ in $N_{TOT}$ may be as high as 89.6%, with PNC between 7,454 ± 4,316 # $cm^{-3}$ (2020) and 9,659 ± 5,031 # $cm^{-3}$ (2022) in the 8–400 nm diameter range. The same proportion has already been observed in previous studies performed in urban background sites

**Table 1.** Average hourly median, mean, minimum and maximum PNC (# $cm^{-3}$) for $N_{UFP}$ (8–100 nm), and $N_{TOT}$ (8–400 nm) measured in Paris over the period and for the years 2020, 2021, and 2022. "n" corresponds to the number of samples considered and Std correspond to the mean standard deviations.

| | | Over the all period (n = 28 512) | 2020 (n = 8 784) | 2021 (n = 8 760) | 2022 (n = 8 759) |
|---|---|---|---|---|---|
| $N_{UFP}$ (# $cm^{-3}$) | Median | 7,037 | 5,791 | 7,156 | 7,775 |
| | **Mean** | **8,082** | **6,552** | **8,115** | **8,734** |
| | **Std** | **4,772** | **3,910** | **4,588** | **4,691** |
| | Min. | 482 | 587 | 482 | 662 |
| | Max. | 38,982 | 30,742 | 36,314 | 37,969 |
| $N_{TOT}$ (# $cm^{-3}$) | Median | 7,929 | 6,629 | 8,094 | 8,621 |
| | **Mean** | **9,021** | **7,454** | **9,083** | **9,659** |
| | **Std** | **5,145** | **4,316** | **4,970** | **5,031** |
| | Min. | 516 | 700 | 516 | 734 |
| | Max | 40,113 | 33,724 | 38,888 | 39,577 |
| $N_{UFP}/N_{TOT}$ (%) | **Mean** | **89.6** | **87.9** | **89.3** | **90.4** |

(Airparif, 2022a; Baldauf *et al.*, 2016; Dall'Osto *et al.*, 2013; Gani *et al.*, 2020; Solomon, 2012; Sun *et al.*, 2019; Trechera *et al.*, 2023). The differences recorded between the lowest (500 and 700 # $cm^{-3}$) and highest (30,000 and 40,000 # $cm^{-3}$) concentrations illustrate the considerable variability in hourly average $N_{UFP}$ and $N_{TOT}$ levels, compared to that usually observed for $PM_{10}$ and $PM_{2.5}$ mass concentrations (Airparif, 2022a, 2022b). In addition, WHO Air Quality Guidelines state that high $N_{TOT}$ concentrations can guide decisions on priorities for controlling UFP emission sources, when daily and hourly averages exceed 10,000 # $cm^{-3}$ or 20,000 # $cm^{-3}$ respectively (WHO, 2021). The WHO daily informative value was exceeded during 353 days, around one-third of the studied period. Therefore, this study shows that measurements in the Paris supersite can be characterized by high $N_{TOT}$ compared to WHO guidelines.

The analysis of averaged annual $N_{UFP}$ indicated lower concentrations in 2020 compared to 2021 and 2022 (Table 1). An increase in UFP concentrations of around 25% has been found between 2020 and 2022. This was more pronounced between 2020 and 2021 (+19%) than between 2021 and 2022 (+7%). This finding may be partly explained by the COVID-19 pandemic and the gradual return to a pre-pandemic situation. However, the associated impact study on $N_{UFP}$ could not be assessed due to the lack of historical data (first UFP measurements on site in October 2019).

As the variability of pollutant concentrations is also depending on meteorological conditions, it was necessary to estimate $N_{UFP}$ by applying the dispersion normalization method (see sub-section 2.4, Eqs. (2–3)). During the studied period, a $N_{UFPnorm}$ value of 7,191 # $cm^{-3}$ was calculated. This may vary between 6,584 # $cm^{-3}$ (2020), 6,653 # $cm^{-3}$ (2021), and 7,660 # $cm^{-3}$ (2022). A less marked increase in $N_{UFPnorm}$ was thus observed between 2020 and 2022 (+13% *versus* +25% with $N_{UFP}$).

In the same way, $N_{UFPnorm}/N_{UFP}$ ratios (calculated on the basis of annual $N_{UFP}$ averages) showed respective values of 1.0, 0.82, and 0.88 for 2020, 2021, and 2022, thus highlighting a stronger impact of weather conditions for pollutant accumulation in 2021 and 2022.

## 3.3 Temporal Evolution of UFP Number Concentrations ($N_{UFP}$)

A significant variability in daily averaged UFP concentrations ranging from 1,500 to 19,000 # $cm^{-3}$ was observed from October 2019 to December 2022 (Fig. 3, in grey). High daily $N_{UFP}$ concentrations ($\geq$ 15,000 # $cm^{-3}$) were recorded during a couple of days at the beginning of the sampling period. As ambient temperatures gradually decline in autumn and winter seasons, an increase in UFP emissions related to a greater use of residential heating was added to emissions from road-traffic, combined with meteorological conditions favorable to the accumulation of locally emitted pollutants (Airparif, 2022a). In this way, highest $N_{UFP}$ monitored during this period were associated with low $VC_{norm}$ ($<$ 1.0) (Fig. 2). Conversely, high $N_{UFP}$ concentrations were observed in warmer months with $VC_{norm} > 1$, more prominently in summer 2020 due to photochemical reactions, i.e., secondary aerosols formation.

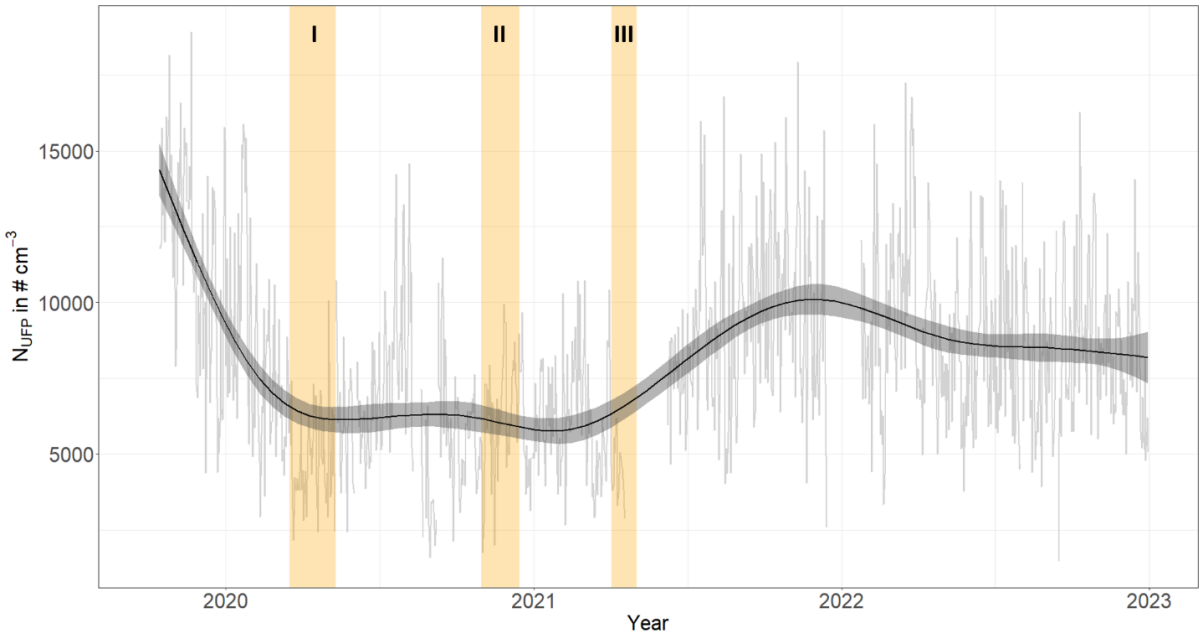


**Fig. 3.** Evolution of the daily average $N_{UFP}$ concentrations from October 2019 to December 2022 (in grey). The black curve represents the smooth-trend curve of the data and the shaded areas show the 95$^{th}$ confidence intervals of the fit. Orange zones illustrate the related-COVID 19 lockdown periods in France (I: from March, 17$^{th}$ to May, 11$^{th}$ 2020; II: from October, 30$^{th}$ to November, 15$^{th}$ 2020; III: from April, 3$^{rd}$ to May, 3$^{rd}$ 2021).

The smooth-trend curve, displayed from rolling monthly averaged UFP data (Fig. 3, in black), highlights that 2020 was an atypical year with high $N_{UFP}$ at the beginning which gradually declined until the first COVID-19 lockdown was implemented. A sharper decrease in UFP concentrations was found at that time in response to policy decisions (e.g., reduction of economic activities and mobility). From that period, the black curve illustrates a "plateau" until the end of the same year due to successive fluctuations between high and low averaged daily $N_{UFP}$ concentrations. During the 2$^{nd}$ national lockdown (with fewer restrictions), daily $N_{UFP}$ were in the same order of magnitude than those monitored in the first half of 2021. A significant increase in $N_{UFP}$ concentrations was then evidenced from the second half of 2021, thus coinciding with the return to normal post-pandemic activities and seasonal emissions (such as residential heating). Similar $N_{UFP}$ concentrations were observed until the end of the year 2022.

Figs. 4(a), 4(b), and 4(c) present the averaged daily, weekly and monthly $N_{UFP}$ concentrations at the Paris-Les Halles supersite for the years 2020, 2021, and 2022. Hourly $N_{UFP}$ profiles (Fig. 4(a)) showed elevated concentrations in the morning (between 6 am and 12 pm), then lower ones in the afternoon (minimum recorded at 3 pm), and finally the highest concentrations in the evening (between 6 pm and 11 pm). This diurnal pattern is consistent with those observed in urban background sites (Airparif, 2022a; Trechera *et al.*, 2023) and corresponds to morning and evening rush hours, and therefore to enhanced local anthropogenic emissions. More intense $N_{UFP}$ concentrations in the evening than in the morning were due to primary emissions, as well as lower photochemical reactions and atmospheric dynamics (with a lower BLH leading to accumulation phenomena). Conversely, lowest $N_{UFP}$ have been noticed at night (from midnight to 6 am) and in the afternoon, due to both less anthropogenic activities and more dispersive meteorological conditions with $VC_{norm}$ values > 1 (maxima at 3 pm, Fig. S1).

However, significant differences in intensity of $N_{UFP}$ concentrations were noticeable. In 2020, lowest and highest daily average levels were less intense (4,000–6,000 # cm$^{-3}$ and 8,000–10,000 # cm$^{-3}$, respectively) than in 2021 and 2022 (5,000–8,000 # cm$^{-3}$ and 10,000–14,000 # cm$^{-3}$, respectively). This finding may also be linked to the context of COVID-19 restrictions.

$N_{UFP}$ concentrations varied over the week (Fig. 4(b)) with higher concentrations between Wednesday and Friday and lower ones on Saturday and Sunday, representing a characteristic

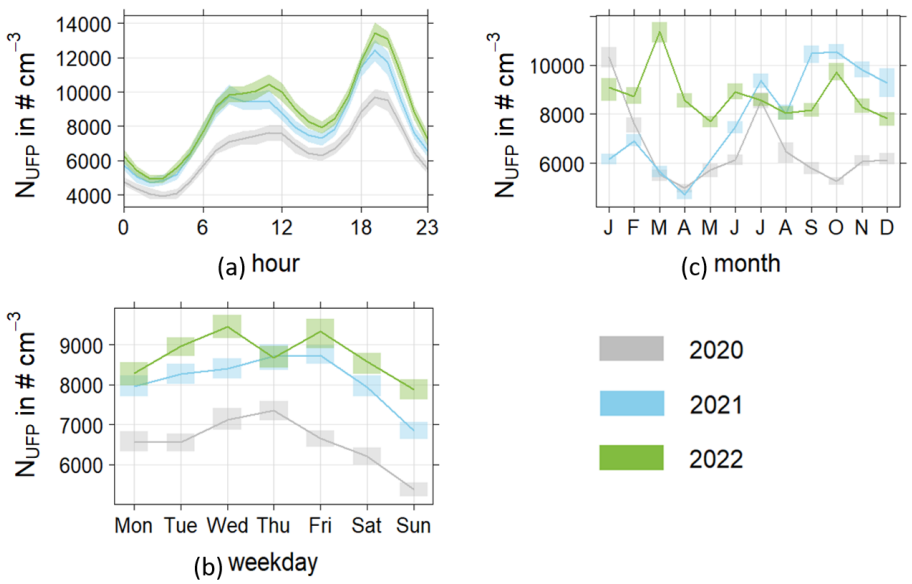


**Fig. 4.** (a) Averaged daily, (b) weekly, and (c) monthly $N_{UFP}$ concentrations at the Paris-Les Halles supersite for the years 2020, 2021, and 2022. Shaded areas indicate the 95$^{th}$ confidence intervals of the mean. For readability purposes, graphics are not on the same scale in terms of concentrations.

cycle of anthropogenic activities into urban areas (Gani *et al.*, 2021; Straaten and Weber, 2021; Khoder and Hassan, 2008). The weekday/weekend ratios showed a decrease of around 15% in 2020, 12% in 2021, and 6% in 2022 on weekends, thus reflecting the impact of human activities associated to road-traffic in UFP concentrations. Indeed, this annual variation is still consistent with that observed from loop-based counting systems (considered as a relevant traffic flow indicator) located near the sampling site and provided by the municipality of Paris (31%, 29%, 24% for respective years) (Paris Opendata, 2024).

Finally, it is worth noting that no clear monthly or seasonal trends in $N_{UFP}$ concentrations were observed over the study period (Fig. 4(c)). This result can be mainly explained by differences in the emission sources and processes allowing particle dispersion and/or formation. Local UFP production can be high in autumn and winter due to combustion processes (road-traffic, domestic heating, …), according to the meteorological context (with colder or milder temperatures) and atmospheric dispersion. In spring and summer, intense sunshine and high temperatures can favor the new particle formation (NPF) (Bousiotis *et al.*, 2021; Rose *et al.*, 2021; Sun *et al.*, 2019). Specific events, such as the heat wave occurring in March 2022, also contributed to the production of secondary aerosols.

## 3.4 Insight of UFP Emission Sources in Paris

Several studies have already examined the relationships between UFP and other gaseous and particulate compounds (Beevers *et al.*, 2012; Grundström *et al.*, 2015; Johansson *et al.*, 2007; Morawska *et al.*, 1998; Rodríguez and Cuevas, 2007; Sánchez Jiménez *et al.*, 2012; Shi *et al.*, 2001; Sun *et al.*, 2019; Trechera *et al.*, 2023; Wu *et al.*, 2015), thus allowing to provide a first overview of the major UFP sources.

For BC, a positive correlation with UFP (Pearson correlation coefficient (PCC) = 0.50) has been found over the whole analysis period (Fig. 5). This value was of the same order of magnitude than UFP with $BC_{ff}$ ($r$ = 0.51). However, the correlation was lower with $BC_{wb}$ ($r$ = 0.33). These findings thus reflect the greater influence of road-traffic emissions compared to wood-burning emissions in Paris. Although these two sources were clearly identified as major UFP emitters, their PCC values were still moderate. This can be explained by the fact that, unlike BC, UFP have very little mass but are present in very high numbers in the atmosphere, thus confirming the observations issued from temporal profiles. Moreover, the comparison of $N_{UFP}$ and BC profiles showed good consistency for the morning (from 6 am to 8 am) and evening peaks, that can be easily associated

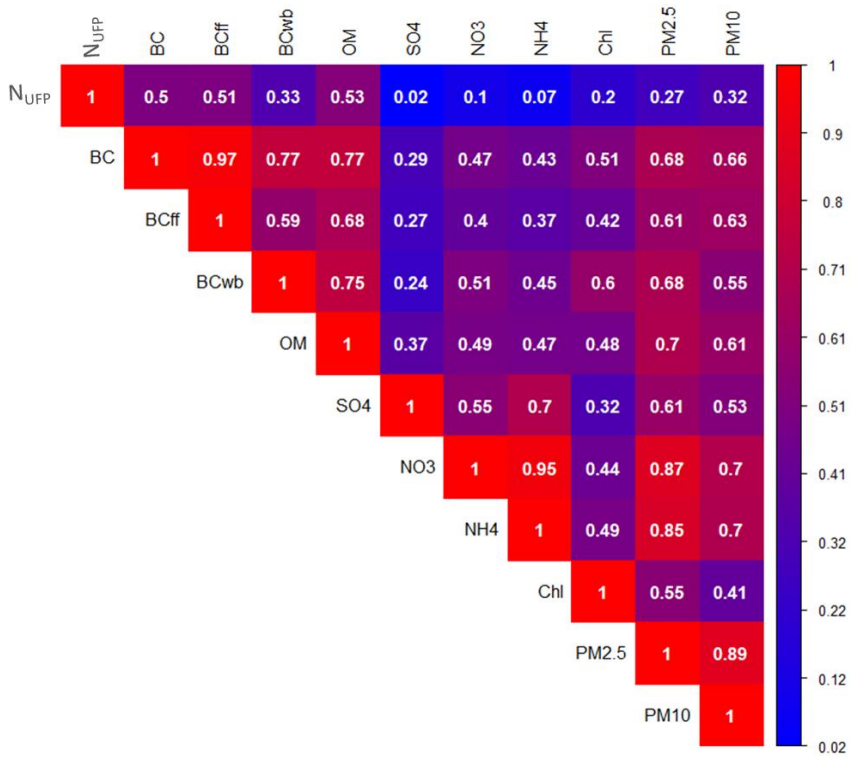


**Fig. 5.** Pearson's correlation coefficient ($r$) of $N_{UFP}$ with particulate matter, including Black Carbon (BC), Black Carbon derived from fossil-fuel ($BC_{ff}$) and wood-burning ($BC_{wb}$) combustion, organic matter (OM), sulfate ($SO_4$), nitrate ($NO_3$), ammonium ($NH_4$), chloride (Chl), $PM_{2.5}$, and $PM_{10}$ with a $p$-value $\leq 0.05$.

with local anthropogenic emissions. The daily variability of $N_{UFP}$ in the late morning did not coincide with that of BC (Fig. S2(a)), thus indicating the presence of other sources in an urban environment. Indeed, this mid-day UFP peak is attributed to the formation of new particles from regional and urban photochemical processes (Trechera *et al.*, 2023).

For OM, a moderate correlation ($r$ = 0.53) was also observed with $N_{UFP}$. Indeed, organic matter can be categorized into either primary organic aerosols, directly emitted from anthropogenic (from incomplete combustion processes) and biogenic sources, or secondary organic aerosols resulting from gas-particle conversions. Sulfate, nitrate and ammonium ions ($SO_4$, $NO_3$, $NH_4$) represent major PM inorganic compounds (Favez *et al.*, 2021; Petit *et al.*, 2015) and are also formed from nucleation processes involving gaseous precursors. For these components, poor correlations with $N_{UFP}$ ($r$ = 0.02–0.1) were found. This finding also showed that $N_{UFP}$ concentrations do not necessarily exhibit the same behaviour as $PM_{10}$ and $PM_{2.5}$ mass concentrations. The correlations between $N_{UFP}$ and $PM_x$ were positive and moderately low ($r$ = 0.32 for $PM_{10}$ and $r$ = 0.27 for $PM_{2.5}$). de Jesus *et al.* (2019) also found low correlations with $PM_{2.5}$ in a global study involving ten cities located in the North America, Europe, Asia, and Australia.

About gaseous compounds, a moderate positive correlation was reached between $NO_2$ and $N_{UFP}$ ($r$ = 0.58) (Fig. 6). This PCC was broadly comparable to that identified in Cattani *et al.* (2017) ($r$ = 0.62) and is in the same order of magnitude than BC, since both compounds are predominantly emitted from fossil fuel combustion processes. NO and $NO_x$ presented lower correlations ($r$ = 0.5 and 0.34, respectively) with $N_{UFP}$. As for $NO_2$, CO is a primary pollutant resulting from incomplete combustion, regardless of the type of fuel used. The relationship between $N_{UFP}$ and CO was still positive and moderately low ($r$ = 0.36) than $NO_2$. Correlations of $N_{UFP}$ with $CO_2$ and $CH_4$ were also low ($r$ = 0.22 and 0.15, respectively). As with $NH_3$, a low PCC was found ($r$ = 0.24) and was however higher than $NH_4$ ($r$ = 0.07). Only ozone displayed a negative correlation with $N_{UFP}$ ($r$ = –0.24). Except for $NO_2$, the presence of these other gases did not allow to characterize a common emission source with UFP.

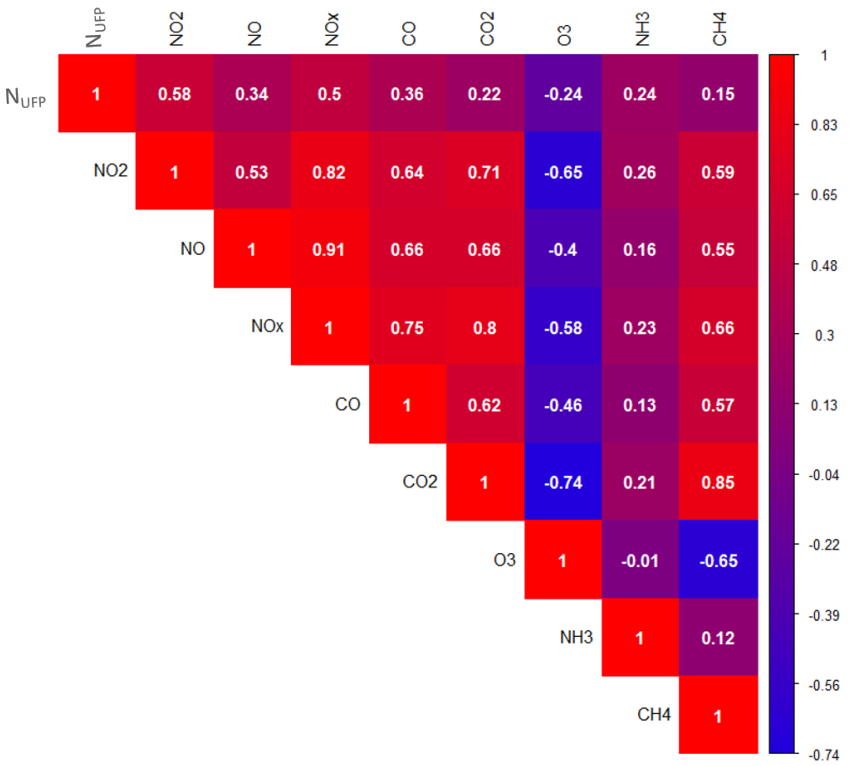


**Fig. 6.** Pearson's correlation coefficient ($r$) of $N_{UFP}$ with gaseous compounds, including nitrogen dioxide ($NO_2$), monoxide (NO) and oxides ($NO_x$), carbon monoxide (CO), carbon dioxide ($CO_2$), ozone ($O_3$), ammonia ($NH_3$), and methane ($CH_4$), with a $p$-value $\leq 0.05$.

Finally, $N_{UFP}$ and meteorological parameters (such as ambient temperature, wind speed and direction, BLH and VC) were very poorly correlated ($r$ ranging from –0.21 to 0.06) (Fig. S3), making impossible to demonstrate a direct and clear connection between meteorology and UFP by considering the whole sampling period. These PCC could be more significant if more restrictive time periods are considered for analyses.

## 3.5 Particle Number Size Distributions

The averaged 3-years PNSD measured at the Paris-Les Halles supersite highlighted a major modal diameter around 25 ± 10 nm (Fig. 7). This particle size range is usually attributed to the Aitken mode and reflects both the growth of particles formed from ambient-temperature gas-to-particle conversion (nucleation processes) and particles directly emitted by combustion processes and more particularly by the road-traffic source (Harrison *et al.*, 2019, 2011; Ogulei *et al.*, 2006). These results emphasized that road-traffic can be considered as a major contributor to UFP emissions in Paris in 2020, 2021, and 2022. This finding was consistent with the conclusions of Trechera *et al.* (2023), regarding similar PNSD profiles measured in European cities such as London and Madrid.

To a slightly lesser extent, another population of particles could be observed between 200 and 300 nm and would be associated to secondary particles with a diameter range included in the accumulation mode (Gu *et al.*, 2011; Rivas *et al.*, 2020).

In addition to the modal diameter, PNSD can also be characterized in terms of median and mean $d_{me}$ (Table 2). The analysis of PNSD allowed to show that mode and median diameters were smaller in 2021 and 2022 (22–23 nm and 29 nm) than in 2020 (27 nm and 32 nm, respectively). This difference in particle size between 2020 and 2022 is more visible for the mean diameter (50 nm versus 44 nm). These three parameters globally showed diameters of 20 to 50 nm.

The highest uncertainties were only recorded for the modal diameter (26–27%). However, they were narrower for median and mean $d_{me}$ (from 3% to 6% and 4%, respectively).

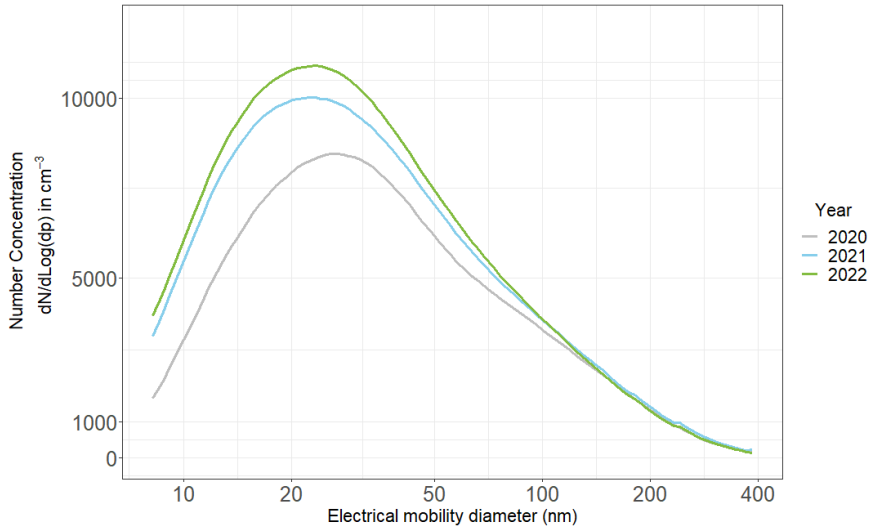


**Fig. 7.** Averaged 2020–2021–2022 particle number size distributions at the Paris-Les Halles supersite in the 8–400 nm electrical mobility size range.

**Table 2.** Statistical diameters (in terms of electrical mobility diameter ($d_{me}$)) calculated from average particle size number distributions (mode, median and mean diameters) for 2020, 2021, and 2022 years. Uncertainties correspond to reproducibility standard deviations ($STD_R$) calculated according to ISO 5725-2 standard.

| $d_{me}$ | 2020 | | 2021 | | 2022 | |
|---|---|---|---|---|---|---|
| | Average (nm) | $STD_R$ (nm) | Average (nm) | $STD_R$ (nm) | Average (nm) | $STD_R$ (nm) |
| Modal | 27 | ±7 | 22 | ±6 | 23 | ±6 |
| Median | 32 | ±2 | 29 | ±1 | 29 | ±1 |
| Mean | 50 | ±2 | 47 | ±2 | 44 | ±2 |

### 3.5.1 Nucleation mode ($N_{nuc} = N_{8\text{-}20}$)

The averaged nucleation-mode particle concentration ($N_{nuc}$) was characterized by a value of 2,794 ± 1,966 # $cm^{-3}$ over the studied period, varying between 1,978 (2020) and 3,125 # $cm^{-3}$ (2022). The analysis of particle number concentrations ranging from 8 to 20 nm showed an increase of 37% between 2020 and 2022 (+31% between 2020 and 2021 and +9% between 2021 and 2022). It further illustrates a more visible impact of restrictive measures occurring in 2020 in the nucleation-mode particle concentrations. Indeed, these particles are mainly emitted by local pollution sources (such as road-traffic in urban areas) and driven by gas-to-particle conversion processes. Since they have a very short lifespan (i.e., in the order of minutes) due to their rapid coagulation or random impaction on surfaces, the evolution in the nucleation-mode particles concentrations can be considered as a relevant indicator for specifically characterizing the fresh-particles emissions which were lower during the COVID-19 pandemic.

During the study period, the nucleation-mode particles concentrations accounted for around 30% of the total measured particle number concentrations ($N_{TOT}$). The correlations of $N_{nuc}$ with auxillary pollutants were broadly low (PCC < 0.4) (Fig. S4). Highest correlations were recorded with $NO_2$ ($r$ = 0.37) and to a lesser extent with $NO_x$, OM, BC, and $BC_{ff}$ (0.27 > $r$ > 0.2), thus highlighting the influence of road-traffic in the nucleation mode.

### 3.5.2 Aitken mode ($N_{Ait} = N_{20\text{-}100}$)

The averaged Aitken-mode particle concentration ($N_{Ait}$) was characterized by a value of 5,288 ± 3,276 # $cm^{-3}$ over the whole sampling period, varying annually between 4,574 (2020) and 5,610 # $cm^{-3}$ (2022). As for the nucleation mode, the evolution of concentrations for particles ranging from 20 to 100 nm also showed an increase of 19% between 2020 and 2022. This percentage is

broadly consistent with that observed for $N_{UFP}$ (see sub-section 3.2). It also should be noted that the Aitken-mode particles concentrations accounted for almost 60% of $N_{TOT}$, i.e., 8–400 nm, further emphasizing the fact that most of particle number concentrations measured in Paris were associated with this particle mode. This analysis confirms the urban background environment of the monitoring site since this station is located far from any direct source of pollution. Therefore, it is rather representative of UFP pollution from the growth of aerosol particles by condensation and coagulation phenomena, initially emitted in the nucleation mode.

For $N_{UFP}$, correlations are slightly higher with $N_{Ait}$ ($r$ = 0.95) than $N_{nuc}$ ($r$ = 0.85) (Fig. S3). Highest PCC of $N_{Ait}$ were found with BC, and in particular with its fossil-fuel fraction ($r$ = 0.61)—compared with its wood-burning fraction ($r$ = 0.42)—and with organic matter ($r$ = 0.63). In addition, $PM_x$ were better correlated with $N_{Ait}$ than $N_{UFP}$, although their correlations were globally low ($r$ = 0.35 and $r$ = 0.42 for $PM_{2.5}$ and $PM_{10}$, respectively). Sulfate, nitrate and ammonium ions ($SO_4$, $NO_3$, $NH_4$) showed very poor correlations with $N_{Ait}$ ($0.07 < r < 0.24$) (Fig. S5, left panel).

Concerning gaseous compounds, $N_{Ait}$ showed the strongest correlations with nitrogen oxides, particularly with $NO_2$ ($r$ = 0.62). A slightly higher correlation was found with CO ($r$ = 0.44). The remaining gases considered in this study presented poor PCC ($r$ below 0.4), even a negative correlation for $O_3$ ($r$ = –0.24). (Fig. S5, right panel). As for $N_{UFP}$, very weak correlations were also found with meteorological parameters.

### 3.5.3 Accumulation mode ($N_{100\text{-}400}$)

The accumulation-mode particles concentrations ($N_{acc}$), corresponding to the 100–400 nm size range, accounted for only 10% of $N_{TOT}$. The averaged particle number concentration recorded in this mode during the whole measurement period was of 939 ± 700 # $cm^{-3}$, with stable values in 2020, 2021, and 2022 (902, 968, and 924 # $cm^{-3}$). The annual differences represented less than 1% of $N_{TOT}$ concentrations, which is not meaningful regarding to those recorded in the two other modes.

The accumulation mode ($N_{acc}$) presented the highest correlations both with particulate and gaseous components (Fig. S6). Indeed, it was the only particle mode which displayed strong correlations with BC ($r$ = 0.85) and organic matter ($r$ = 0.83), $N_{acc}$ being better correlated with $BC_{wb}$ ($r$ = 0.82) than $BC_{ff}$ ($r$ = 0.77). These results perfectly illustrate that primary UFP sources are mainly related to road-traffic activities and that biomass combustion emissions have also a significant contribution on the UFP size range but also on larger particles diameters (> 100 nm). This principle also applies for secondary inorganic aerosols. After being formed in the nucleation mode, these compounds rapidly grow in the Aitken and then the accumulation modes. That is the reason why moderate correlations of $N_{acc}$ with $NO_3$ and $NH_4$ ($r$ = 0.56 and $r$ = 0.52, respectively) were found. However, PCC remained weaker for $SO_4$ and Chl ($r$ = 0.34 and $r$ = 0.43), since these compounds have lower mass contributions than ammonium nitrate ones.

Contrary to the first two particle modes, the accumulation mode displayed strong correlations with $PM_{2.5}$ and $PM_{10}$ ($r$ = 0.77 and $r$ = 0.69, respectively). This result highlights that the accumulation mode contributed significantly to $PM_{10}$ and $PM_{2.5}$ mass concentrations although they were far less numerous than $N_{UFP}$ (Kwon *et al.*, 2020). $N_{acc}$ were well correlated with gaseous compounds, with coefficients that can however be weakly to strongly moderated ($0.4 < r < 0.7$). As for $N_{nuc}$ and $N_{Ait}$, the accumulation mode also showed a negative coefficient with ozone ($r$ = –0.32).

## 3.6 Comparison of UFP Concentrations Observed in Paris with the Literature

The RI-URBANS project (Research Infrastructures Services Reinforcing Air Quality Monitoring Capacities in European Urban & Industrial Areas, the European Union's Horizon 2020 research and innovation program, n°101036245) allowed to gather and evaluate available UFP/PNC data from urban areas in several countries and to conduct comparisons with these concentrations. In the absence of a Paris' urban site for the aforementioned study, any comparison could not be made and is then carried out in this paper.

The averaged number concentrations of particles ranging from 10 to 25 nm ($N_{10\text{-}25}$), from 25 to 100 nm ($N_{25\text{-}100}$) and from 10 to 100 nm ($N_{10\text{-}100}$, representative of UFP size range) observed in Paris in 2022 were compared to those measured in fifteen European cities (+1 in the USA) over the 2017–2019 period (Table 3). The decision to lead this comparison for the year 2022 was

guided by the fact that a normal return of anthropogenic activities (representative of the emissions intensity before the pre-pandemic period) was occurred. This study thus establishes a reliable and relevant comparison with concentrations measured before 2020.

The highest $N_{UFP}$ concentrations were recorded in Barcelona, Granada, Langen, Budapest, Marseille, Paris and Mülheim (7,868–9,805 # $cm^{-3}$), followed by Athens, Madrid, Leipzig and Dresden (4,973–6,841 # $cm^{-3}$) and Rochester, Helsinki, London_1, London_2, Zurich and Birmingham (2,858–3,804 # $cm^{-3}$).

For $N_{10\text{-}25}$ concentrations, they were globally from 540 to 4,628 # $cm^{-3}$, with highest number concentrations in Central, Eastern and South-Western Europe (2,800–4,600 # $cm^{-3}$, including Paris (3,688 # $cm^{-3}$)) and lowest levels in northern Europe, in the UK and in the northern USA (700–1,400 # $cm^{-3}$, except for Zurich with 300 # $cm^{-3}$). This spatial distribution in the $N_{10\text{-}25}$ concentrations can be associated to cities located in southern Europe and mainly affected by photo-nucleation processes favored by intense temperature and sunshine conditions. In addition, other contributors such as the road-traffic emission source and various physico-chemical processes can also affect the number particle concentrations in this particle size range.

For $N_{25\text{-}100}$ concentrations, the averaged particle number concentrations recorded in urban background conditions were from 2,144 to 5,894 # $cm^{-3}$. As for Trechera *et al.* (2023), it is important to note that marked South-Center-North (S-C-N) $N_{25\text{-}100}$ trends were observed, with the higher concentrations in southern Europe, notably in Madrid, Athens, Barcelona and Marseille (4,800–5,900 # $cm^{-3}$), and then intermediate number concentrations (2,800–5,100 # $cm^{-3}$) were found in Zurich, Leipzig, Mülheim, Budapest and Paris ($N_{25\text{-}100}$ = 4,591 # $cm^{-3}$). The lowest particle levels were again recorded in Northern Europe, in the UK and in the northern USA (2,100–3,000 # $cm^{-3}$).

Relatively high number particle concentrations within $N_{UFP}$, $N_{10\text{-}25}$, $N_{25\text{-}100}$ (8,300, 3,700, and 4,600 # $cm^{-3}$, respectively) were found in Paris and can mostly be associated with emissions from road-traffic (also confirmed by the correlation study, see sub-sections 3.4 and 3.5), as for other European cities with similar characteristics. However, it is also important to mention that particle-counting monitoring technologies used in these studies may differ from one city to another, thus leading to balance some elements of this comparison. Indeed, this lack of harmonization in terms of instrumentation, calibration chain and data processing should soon be standardized to make these analyses strictly comparable.

**Table 3.** Averaged particles number concentrations and their standard deviations for $N_{10\text{-}25}$, $N_{25\text{-}100}$, $N_{10\text{-}100}$ ($N_{UFP}$) from 16 urban background sites (2017–2019 period, Trechera *et al.*, 2023) compared to Paris (year 2022).

| Station name | $N_{10\text{-}25}$ (# $cm^{-3}$) | $\sigma_{10\text{-}25}$ (# $cm^{-3}$) | $N_{25\text{-}100}$ (# $cm^{-3}$) | $\sigma_{25\text{-}100}$ (# $cm^{-3}$) | $N_{UFP}$ ($N_{10\text{-}100}$) (# $cm^{-3}$) | $\sigma_{10\text{-}100}$ (# $cm^{-3}$) |
|---|---|---|---|---|---|---|
| This work (Paris) | 3,688 | 2,301 | 4,591 | 2,701 | 8,279 | 4,530 |
| Athens | 1,503 | 1,312 | 5,338 | 4,642 | 6,841 | 5,448 |
| Barcelona | 4,245 | 4,141 | 5,560 | 3,820 | 9,805 | 6,641 |
| Birmingham | 661 | 632 | 2,197 | 1,813 | 2,858 | 2,263 |
| Budapest | 3,691 | 3,075 | 4,973 | 3,333 | 8,664 | 5,785 |
| Dresden | 1,935 | 2,322 | 3,038 | 2,529 | 4,973 | 4,019 |
| Granada | 3,129 | 2,677 | 5,629 | 4,160 | 8,758 | 6,230 |
| Helsinki | 1,419 | 1,526 | 2,144 | 1,764 | 3,563 | 2,913 |
| Langen | 4,628 | 4,491 | 4,074 | 2,762 | 8,702 | 5,890 |
| Leipzig | 3,236 | 4,076 | 3,524 | 2,818 | 6,760 | 5,691 |
| London_1 | 614 | 560 | 2,983 | 2,433 | 3,597 | 2,790 |
| London_2 | 540 | 405 | 2,912 | 2,256 | 3,452 | 2,509 |
| Madrid | 1,997 | 1,908 | 4,806 | 3,632 | 6,803 | 4,942 |
| Marseille | 2,679 | 1,760 | 5,894 | 3,881 | 8,573 | 5,160 |
| Mülheim | 2,810 | 2,139 | 5,058 | 3,375 | 7,868 | 4,955 |
| Rochester | 1,434 | 1,428 | 2,370 | 1,849 | 3,804 | 2,867 |
| Zürich | 296 | 264 | 2,845 | 2,156 | 3,141 | 2,336 |

## 4 CONCLUSIONS

Since October 2019, continuous ultrafine particles (UFP) measurements were performed at an urban background supersite in Paris using an electric mobility particle size spectrometer (MPSS), thus complying with the WHO recommendations and the future EU air quality directive. In this study, UFP data were collected until December 2022. The results revealed high UFP number concentrations compared to other major cities, with an hourly averaged value of 8,100 ± 4,800 # $cm^{-3}$ over the study period. The annual concentrations could fluctuate from 6,600 ± 3,900 # $cm^{-3}$ in 2020 to 8,700 ± 4,700 # $cm^{-3}$ in 2022. Hourly maximum UFP concentrations reached 30,000 and 40,000 # $cm^{-3}$. The WHO daily informative value (i.e., $N_{TOT}$ with $N_{UFP}$ included > 10,000 # $cm^{-3}$) was then exceeded during 353 days, around one-third of the studied period. These results indicate that Paris city is one of the European cities mostly affected by UFP pollution, thus underlining the need to implement effective air quality management strategies.

This study also highlighted the important variability in UFP number concentrations, in comparison with $PM_{10}$ and $PM_{2.5}$ mass concentrations. An expected daily pattern was identified with high concentrations in the morning and evening rush-hour periods mainly associated to anthropogenic activities, especially road-traffic. Additional UFP peak concentration was observed at mid-day and can be attributed to the formation of new particles from nucleation processes. These phenomena contribute to the complexity in the UFP understanding and their dynamics within the greater Paris area. Moreover, no clear monthly or seasonal UFP variability was observed.

Correlations of UFP with other pollutants varied generally from weak to moderate, with highest relationships obtained with combustion pollutants, such as $NO_2$ ($r$ = 0.58) and BC, more particularly from fossil fuel ($BC_{ff}$, $r$ = 0.51) whereas UFP showed a weaker correlation with the wood-burning source ($BC_{wb}$, $r$ = 0.33). In addition, the analysis of particle number size distributions (PNSD) allowing to characterize the relative contributions of nucleation, Aitken and accumulation modes to the whole measured size range (i.e., 8–400 nm) were about 30%, 60%, and 10%, respectively. This confirmed that road traffic was the main UFP source in Paris since the Aitken mode was mainly correlated to BC and its fossil-fuel fraction.

Since April 2022, the MPSS and CNC-combined particle monitoring, in addition to existing real-time measurements of the aerosol chemical composition, should further improve the understanding of UFP sources and formation mechanisms. A long-term analysis of UFP data will allow to better characterize their main sources and identify specific events influencing UFP number concentrations. The understanding of UFP spatio-temporal variabilities and the analysis of PNSD profiles are worthwhile to implement effective air quality management plans and support policy decisions aimed at controlling UFP emissions, especially within the greater Paris area. Such particle number concentrations monitoring has also recently been completed by oxidative potential measurements to refine knowledge of the impact of particulate matter on human health.

## SUPPLEMENTARY MATERIAL

Supplementary material for this article can be found in the online version at https://doi.org/10.4209/aaqr.240093

## ADDITIONAL INFORMATION AND DECLARATIONS

### Conflict of Interest Statement

The authors declare no conflict of interest.

### Data Availability

All the data presented in this paper are available upon request. Please contact Gregory Abbou (gregory.abbou@airparif.fr) or Alexia Baudic (alexia.baudic@airparif.fr) for further information.

## Funding

This work was performed thanks to the Airparif members funding. Moreover, the MPSS involved in this study was funded by the Ile-de-France regional council.

## REFERENCES

ACTRIS (2021). Preliminary ACTRIS recommendation for aerosol in-situ sampling, measurements, and analysis. https://www.actris.eu/sites/default/files/2021-06/Preliminary%20ACTRIS%20recommendations%20for%20aerosol%20in-situ%20measurements%20June%202021.pdf (accessed 02 August 2024).

Agence nationale de sécurité sanitaire, de l'alimentation, de l'environnement et du travail (ANSES) (2019). Effets sanitaires des particules de l'air ambiant extérieur selon les composés, les sources et la granulométrie. Rapport d'expertise collective, Juillet 2019, pp. 97. https://www.anses.fr/fr/system/files/AIR2014SA0156Ra-Sante.pdf (accessed 02 August 2024).

Airparif (2022a). Campagne de mesure francilienne sur les particules ultrafines (UFP) : Situation de fond hiver 2020-2021. https://www.airparif.fr/sites/default/files/document_publication/Synth%C3%A8se_PUF.pdf (accessed 02 August 2024).

Airparif (2022b). Air quality monitoring and information in Île-de-France: regional air quality report - Year 2021. https://www.airparif.fr/sites/default/files/document_publication/BilanQA_IDF_2021_UK.pdf (accessed 02 August 2024).

Baldauf, R., Devlin, R., Gehr, P., Giannelli, R., Hassett-Sipple, B., Jung, H., Martini, G., McDonald, J., Sacks, J., Walker, K. (2016). Ultrafine particle metrics and research considerations: Review of the 2015 UFP workshop. J. Environ. Res. Public Health 13, 1054. https://doi.org/10.3390/ijerph13111054

Beevers, S.D., Westmoreland, E., de Jong, M.C., Williams, M.L., Carslaw, D.C. (2012). Trends in $NO_x$ and $NO_2$ emissions from road traffic in Great Britain. Atmos. Environ. 54, 107–116. https://doi.org/10.1016/J.ATMOSENV.2012.02.028

Bousiotis, D., Pope, F.D., Beddows, D.C.S., Dall'Osto, M., Massling, A., Nøjgaard, J.K., Nordstrøm, C., Niemi, J.V., Portin, H., Petäjä, T., Perez, N., Alastuey, A., Querol, X., Kouvarakis, G., Mihalopoulos, N., Vratolis, S., Eleftheriadis, K., Wiedensohler, A., Weinhold, K., Merkel, M., *et al.* (2021). A phenomenology of new particle formation (NPF) at 13 European sites. Atmos. Chem. Phys. 21, 11905–11925. https://doi.org/10.5194/acp-21-11905-2021

Carslaw, D.C., Ropkins, K. (2012). openair — An R package for air quality data analysis. Environ. Modell. Software 27–28, 52–61. https://doi.org/10.1016/j.envsoft.2011.09.008

Casquero-Vera, J.A., Lyamani, H., Titos, G., Minguillón, M.C., Dada, L., Alastuey, A., Querol, X., Petäjä, T., Olmo, F.J., Alados-Arboledas, L. (2021). Quantifying traffic, biomass burning and secondary source contributions to atmospheric particle number concentrations at urban and suburban sites. Sci. Total Environ. 768, 145282. https://doi.org/10.1016/j.scitotenv.2021.145282

Cassee, F., Morawska, L., Peters, A. (2019). The White Paper on Ambient Ultrafine Particles: evidence for policy makers. 'Thinking outside the box' Team, October 2019, pp. 23. https://efca.net/files/WHITE%20PAPER-UFP%20evidence%20for%20policy%20makers%20(25%20OCT).pdf (accessed 02 August 2024).

Cattani, G., Gaeta, A., Di Menno Di Bucchianico, A., De Santis, A., Gaddi, R., Cusano, M., Ancona, C., Badaloni, C., Forastiere, F., Gariazzo, C., Sozzi, R., Inglessis, M., Silibello, C., Salvatori, E., Manes, F., Cesaroni, G. (2017). Development of land-use regression models for exposure assessment to ultrafine particles in Rome, Italy. Atmos. Environ. 156, 52–60. https://doi.org/10.1016/j.atmosenv.2017.02.028

CEN/TS 16976:2016 (2016). Ambient air - Determination of the particle number concentration of atmospheric aerosol. https://standards.iteh.ai/catalog/standards/cen/91f1ac67-f6d6-408c-af89-e81763194fd3/cen-ts-16976-2016 (accessed 02 August 2024).

CEN/TS 17434:2020 (2020). Ambient air - Determination of the particle number size distribution of atmospheric aerosol using a Mobility Particle Size Spectrometer (MPSS). https://standards.iteh.ai/catalog/standards/cen/a841bc08-ed34-4fa8-94ca-8c5e07b99db9/cen-ts-17434-2020 (accessed 02 August 2024).

CEN/TC 264/WG 32 (2024). Air quality - Determination of the particle number concentration. https://standards.iteh.ai/catalog/tc/cen/7c511ec9-b305-4ba0-9447-12098c9050eb/cen-tc-264-wg-32 (accessed 02 August 2024).

Charron, A., Harrison, R.M. (2003). Primary particle formation from vehicle emissions during exhaust dilution in the roadside atmosphere. Atmos. Environ. 37, 4109–4119. https://doi.org/10.1016/S1352-2310(03)00510-7

Chen, Y., Masiol, M., Squizzato, S., Chalupa, D.C., Zíková, N., Pokorná, P., Rich, D.Q., Hopke, P.K. (2022). Long-term trends of ultrafine and fine particle number concentrations in New York State: Apportioning between emissions and dispersion. Environ. Pollut. 310, 119797. https://doi.org/10.1016/j.envpol.2022.119797

Dall'Osto, M., Querol, X., Alastuey, A., O'Dowd, C., Harrison, R.M., Wenger, J., Gómez-Moreno, F.J. (2013). On the spatial distribution and evolution of ultrafine particles in Barcelona. Atmos. Chem. Phys. 13, 741–759. https://doi.org/10.5194/acp-13-741-2013

de Jesus, A.L., Rahman, M.M., Mazaheri, M., Thompson, H., Knibbs, L.D., Jeong, C., Evans, G., Nei, W., Ding, A., Qiao, L., Li, L., Portin, H., Niemi, J.V., Timonen, H., Luoma, K., Petäjä, T., Kulmala, M., Kowalski, M., Peters, A., Cyrys, J., *et al.* (2019). Ultrafine particles and $PM_{2.5}$ in the air of cities around the world: Are they representative of each other? Environ. Int. 129, 118–135. https://doi.org/10.1016/j.envint.2019.05.021

Directive 2004/107/EC (2004). Directive 2004/107/EC of the European Parliament and of the Council of 15 December 2004 relating to arsenic, cadnium, mercury, nickel and polycyclic aromatic hydrocarbons in ambient air, OJL, 23, 26.1.2005, pp. 3–16. https://eur-lex.europa.eu/eli/dir/2004/107/oj (accessed 02 August 2024).

Directive 2008/50/EC (2008). Directive 2008/50/EC of the European Parliament and of the Council of 21 May 2008 on ambient air quality and cleaner air for Europe, OJL, 152, 11.6.2008, pp. 1–44. https://eur-lex.europa.eu/eli/dir/2008/50/oj (accessed 02 August 2024).

Dudhia, J., Bresch, J.F. (2002). A global version of the PSU–NCAR mesoscale model. Mon. Wea. Rev. 130, 2989–3007. https://doi.org/10.1175/1520-0493(2002)130<2989:AGVOTP>2.0.CO;2

European Parliament (2022). Proposal for a Directive of the European Parliament and of the Council on ambient air quality and cleaner air for Europe (recast), Article 10, under revision – Version 26.10.2022. https://eur-lex.europa.eu/legal-content/EN/TXT/?uri=COM%3A2022%3A542%3AFIN (accessed 02 August 2024).

Favez, O., Weber, S., Petit, J.E., Alleman, L.Y., Albinet, A., Riffault, V., Chazeau, B., Amodeo, T., Salameh, D., Zhang, Y., Srivastava, D., Samaké, A., Aujay-Plouzeau, R., Papin, A., Bonnaire, N., Boullanger, C., Chatain, M., Chevrier, F., Detournay, A., Dominik-Sègue, M., *et al.* (2021). Overview of the French operational network for in situ observation of PM chemical composition and sources in urban environments (CARA program). Atmosphere 12, 207. https://doi.org/10.3390/atmos12020207

Gani, S., Bhandari, S., Patel, K., Seraj, S., Soni, P., Arub, Z., Habib, G., Hildebrandt Ruiz, L., Apte, J.S. (2020). Particle number concentrations and size distribution in a polluted megacity: The Delhi Aerosol Supersite study. Atmos. Chem. Phys. 20, 8533–8549. https://doi.org/10.5194/acp-20-8533-2020

Gani, S., Chambliss, S.E., Messier, K.P., Lunden, M.M., Apte, J.S. (2021). Spatiotemporal profiles of ultrafine particles differ from other traffic-related air pollutants: lessons from long-term measurements at fixed sites and mobile monitoring. Environ. Sci.: Atmos. 1, 558–568. https://doi.org/10.1039/D1EA00058F

Grundström, M., Hak, C., Chen, D., Hallquist, M., Pleijel, H. (2015). Variation and co-variation of $PM_{10}$, particle number concentration, $NO_x$ and $NO_2$ in the urban air – Relationships with wind speed, vertical temperature gradient and weather type. Atmos. Environ. 120, 317–327. https://doi.org/10.1016/j.atmosenv.2015.08.057

Gu, J., Pitz, M., Schnelle-Kreis, J., Diemer, J., Reller, A., Zimmermann, R., Soentgen, J., Stoelzel, M., Wichmann, H.E., Peters, A., Cyrys, J. (2011). Source apportionment of ambient particles: Comparison of positive matrix factorization analysis applied to particle size distribution and chemical composition data. Atmos. Environ. 45, 1849–1857. https://doi.org/10.1016/j.atmosenv.2011.01.009

Harrison, R.M., Beddows, D.C.S., Dall'Osto, M. (2011). PMF analysis of wide-range particle size

spectra collected on a major highway. Environ. Sci. Technol. 45, 5522–5528. https://doi.org/10.1021/es2006622

Harrison, R.M., Beddows, D.C.S., Alam, M.S., Singh, A., Brean, J., Xu, R., Kotthaus, S., Grimmond, S. (2019). Interpretation of particle number size distributions measured across an urban area during the FASTER campaign. Atmos. Chem. Phys. 19, 39–55. https://doi.org/10.5194/acp-19-39-2019

Hopke, P.K., Feng, Y., Dai, Q. (2022). Source apportionment of particle number concentrations: A global review. Sci. Total Environ. 819, 153104. https://doi.org/10.1016/j.scitotenv.2022.153104

Hussein, T., Puustinen, A., Aalto, P.P., Mäkelä, J.M., Hämeri, K., Kulmala, M. (2004). Urban aerosol number size distributions. Atmos. Chem. Phys. 4, 391–411. https://doi.org/10.5194/acp-4-391-2004

ISO 5725-2:1994 (1994). Accuracy (trueness and precision) of measurement methods andresults—Part 2: Basic method for the determination of repeatability and repro-ducibility of a standard measurement method. International Organization for Standardization. https://www.iso.org/obp/ui/#iso:std:iso:5725:-2:ed-2:v1:en (accessed 02 August 2024).

ISO 15900:2020 (2020). Determination of particle size distribution - Differential electrical mobility analysis for aerosol particles. https://www.iso.org/obp/ui/#iso:std:iso:15900:ed-2:v1:en (accessed 02 August 2024).

Jimenez, J.L., Canagaratna, M.R., Donahue, N.M., Prevot, A.S.H., Zhang, Q., Kroll, J.H., DeCarlo, P.F., Allan, J.D., Coe, H., Ng, N.L., Aiken, A.C., Docherty, K.S., Ulbrich, I.M., Grieshop, A.P., Robinson, A.L., Duplissy, J., Smith, J.D., Wilson, K.R., Lanz, V.A., Hueglin, C., *et al.* (2009). Evolution of organic aerosols in the atmosphere. Science 326, 1525–1529. https://doi.org/10.1126/science.1180353

Johansson, C., Norman, M., Gidhagen, L. (2007). Spatial & temporal variations of $PM_{10}$ and particle number concentrations in urban air. Environ. Monit. Assess. 127, 477–487. https://doi.org/10.1007/s10661-006-9296-4

Khoder, M.I., Hassan, S.K. (2008). Weekday/weekend differences in ambient aerosol level and chemical characteristics of water-soluble components in the city centre. Atmos. Environ. 42, 7483–7493. https://doi.org/10.1016/j.atmosenv.2008.05.068

Knibbs, L.D., Cole-Hunter, T., Morawska, L. (2011). A review of commuter exposure to ultrafine particles and its health effects. Atmos. Environ. 45, 2611–2622. https://doi.org/10.1016/j.atmosenv.2011.02.065

Kulmala, M., Vehkamäki, H., Petäjä, T., Dal Maso, M., Lauri, A., Kerminen, V.M., Birmili, W., McMurry, P.H. (2004). Formation and growth rates of ultrafine atmospheric particles: a review of observations. J. Aerosol Sci. 35, 143–176. https://doi.org/10.1016/j.jaerosci.2003.10.003

Kwon, H.S., Ryu, M.H., Carlsten, C. (2020). Ultrafine particles: unique physicochemical properties relevant to health and disease. Exp. Mol. Med. 52, 318–328. https://doi.org/10.1038/s12276-020-0405-1

Ling, Y., Wang, Y., Duan, J., Xie, X., Liu, Y., Peng, Y., Qiao, L., Cheng, T., Lou, S., Wang, H., Li, X., Xing, X. (2019). Long-term aerosol size distributions and the potential role of volatile organic compounds (VOCs) in new particle formation events in Shanghai. Atmos. Environ. 202, 345–356. https://doi.org/10.1016/j.atmosenv.2019.01.018

Maher, B.A., Ahmed, I.A.M., Karloukovski, V., MacLaren, D.A., Foulds, P.G., Allsop, D., Mann, D.M.A., Torres-Jardón, R., Calderon-Garciduenas, L. (2016). Magnetite pollution nanoparticles in the human brain. Proc. Natl. Acad. Sci. U.S.A. 113, 10797–10801. https://doi.org/10.1073/pnas.1605941113

Morawska, L., Thomas, S., Bofinger, N., Wainwright, D., Neale, D. (1998). Comprehensive characterization of aerosols in a subtropical urban atmosphere. Atmos. Environ. 32, 2467–2478. https://doi.org/10.1016/S1352-2310(98)00023-5

Oberdörster, G., Oberdörster, E., Oberdörster, J. (2005). Nanotoxicology: an emerging discipline evolving from studies of ultrafine particles. Environ. Health Perspect. 113, 823–839. https://doi.org/10.1289/ehp.7339

Ogulei, D., Hopke, P.K., Wallace, L.A. (2006). Analysis of indoor particle size distributions in an occupied townhouse using positive matrix factorization. Indoor Air 16, 204–215. https://doi.org/10.1111/j.1600-0668.2006.00418.x

Paris Opendata (2024). Reference loop-based counting: DP00413. https://opendata.paris.fr/explore/dataset/comptages-routiers-permanents/ (accessed 02 August 2024).

Petit, J.E., Favez, O., Sciare, J., Crenn, V., Sarda-Estève, R., Bonnaire, N., Močnik, G., Dupont, J.C., Haeffelin, M., Leoz-Garziandia, E. (2015). Two years of near real-time chemical composition of submicron aerosols in the region of Paris using an Aerosol Chemical Speciation Monitor (ACSM) and a multi-wavelength Aethalometer. Atmos. Chem. Phys. 15, 2985–3005. https://doi.org/10.5194/acp-15-2985-2015

Rivas, I., Beddows, D.C.S., Amato, F., Green, D.C., Järvi, L., Hueglin, C., Reche, C., Timonen, H., Fuller, G.W., Niemi, J.V., Pérez, N., Aurela, M., Hopke, P.K., Alastuey, A., Kulmala, M., Harrison, R.M., Querol, X., Kelly, F.J. (2020). Source apportionment of particle number size distribution in urban background and traffic stations in four European cities. Environ. Int. 135, 105345. https://doi.org/10.1016/j.envint.2019.105345

Rivas, I., Vicens, L., Basagaña, X., Tobías, A., Katsouyanni, K., Walton, H., Hüglin, C., Alastuey, A., Kulmala, M., Harrison, R.M., Pekkanen, J., Querol, X., Sunyer, J., Kelly, F.J. (2021). Associations between sources of particle number and mortality in four European cities. Environ. Int. 155, 106662. https://doi.org/10.1016/j.envint.2021.106662

Rodríguez, S., Cuevas, E. (2007). The contributions of "minimum primary emissions" and "new particle formation enhancements" to the particle number concentration in urban air. J. Aerosol Sci. 38, 1207–1219. https://doi.org/10.1016/j.jaerosci.2007.09.001

Rose, C., Collaud Coen, M., Andrews, E., Lin, Y., Bossert, I., Lund Myhre, C., Tuch, T., Wiedensohler, A., Fiebig, M., Aalto, P., Alastuey, A., Alonso-Blanco, E., Andrade, M., Artíñano, B., Arsov, T., Baltensperger, U., Bastian, S., Bath, O., Beukes, J.P., Brem, B.T., *et al.* (2021). Seasonality of the particle number concentration and size distribution: a global analysis retrieved from the network of Global Atmosphere Watch (GAW) near-surface observatories. Atmos. Chem. Phys. 21, 17185–17223. https://doi.org/10.5194/acp-21-17185-2021

Sánchez Jiménez, A., Heal, M.R., Beverland, I.J. (2012). Correlations of particle number concentrations and metals with nitrogen oxides and other traffic-related air pollutants in Glasgow and London. Atmos. Environ. 54, 667–678. https://doi.org/10.1016/j.atmosenv.2012.01.047

Schraufnagel, D.E., Balmes, J.R., Cowl, C.T., De Matteis, S., Jung, S.H., Mortimer, K., Perez-Padilla, R., Rice, M.B., Riojas-Rodriguez, H., Sood, A., Thurston, G.D., To, T., Vanker, A., Wuebbles, D.J. (2019). Air pollution and noncommunicable diseases: A review by the forum of international respiratory societies' environmental committee, Part 2: Air pollution and organ systems. Chest 155, 417–426. https://doi.org/10.1016/j.chest.2018.10.041

Setyan, A., Song, C., Merkel, M., Knighton, W.B., Onasch, T.B., Canagaratna, M.R., Worsnop, D.R., Wiedensohler, A., Shilling, J.E., Zhang, Q. (2014). Chemistry of new particle growth in mixed urban and biogenic emissions – insights from CARES. Atmos. Chem. Phys. 14, 6477–6494. https://doi.org/10.5194/acp-14-6477-2014

Shi, J.P., Evans, D.E., Khan, A.A., Harrison, R.M. (2001). Sources and concentration of nanoparticles (<10nm diameter) in the urban atmosphere. Atmos. Environ. 35, 1193–1202. https://doi.org/10.1016/S1352-2310(00)00418-0

Solomon, P.A. (2012). An Overview of Ultrafine Particles in Ambient Air. Air & Waste Management Association, Pittsburgh, PA, pp. 18–27.

Straaten, A., Weber, S. (2021). Measurement report: Three years of size-resolved eddy-covariance particle number flux measurements in an urban environment. Atmos. Chem. Phys. 21, 18707–18726. https://doi.org/10.5194/acp-21-18707-2021

Sujatha, P., Mahalakshmi, D.V., Ramiz, A., Rao, P.V.N., Naidu, C.V. (2016). Ventilation coefficient and boundary layer height impact on urban air quality. Cogent Environ. Sci. 2, 1125284. https://doi.org/10.1080/23311843.2015.1125284

Sun, J., Birmili, W., Hermann, M., Tuch, T., Weinhold, K., Spindler, G., Schladitz, A., Bastian, S., Löschau, G., Cyrys, J., Gu, J., Flentje, H., Briel, B., Asbach, C., Kaminski, H., Ries, L., Sohmer, R., Gerwig, H., Wirtz, K., Meinhardt, F., *et al.* (2019). Variability of black carbon mass concentrations, sub-micrometer particle number concentrations and size distributions: results of the German Ultrafine Aerosol Network ranging from city street to High Alpine locations. Atmos. Environ. 202, 256–268. https://doi.org/10.1016/j.atmosenv.2018.12.029

Terzano, C., Di Stefano, F., Conti, V., Graziani, E., Petroianni, A. (2010). Air pollution ultrafine particles: toxicity beyond the lung. Eur. Rev. Med. Pharmacol. Sci. 14, 809–821. https://www.europeanreview.org/wp/wp-content/uploads/824.pdf

Thén, W., Salma, I. (2022). Particle number concentration: A case study for air quality monitoring. Atmosphere 13, 570. https://doi.org/10.3390/atmos13040570

Trechera, P., Garcia-Marlès, M., Liu, X., Reche, C., Pérez, N., Savadkoohi, M., Beddows, D., Salma, I., Vörösmarty, M., Casans, A., Casquero-Vera, J.A., Hueglin, C., Marchand, N., Chazeau, B., Gille, G., Kalkavouras, P., Mihalopoulos, N., Ondracek, J., Zikova, N., Niemi, J.V., *et al.* (2023). Phenomenology of ultrafine particle concentrations and size distribution across urban Europe. Environ. Int. 172, 107744. https://doi.org/10.1016/j.envint.2023.107744

Wiedensohler, A., Birmili, W., Nowak, A., Sonntag, A., Weinhold, K., Merkel, M., Wehner, B., Tuch, T., Pfeifer, S., Fiebig, M., Fjäraa, A.M., Asmi, E., Sellegri, K., Depuy, R., Venzac, H., Villani, P., Laj, P., Aalto, P., Ogren, J.A., Swietlicki, E., *et al.* (2012). Mobility particle size spectrometers: harmonization of technical standards and data structure to facilitate high quality long-term observations of atmospheric particle number size distributions. Atmos. Meas. Tech. 5, 657–685. https://doi.org/10.5194/amt-5-657-2012

Wiedensohler, A., Wiesner, A., Weinhold, K., Birmili, W., Hermann, M., Merkel, M., Müller, T., Pfeifer, S., Schmidt, A., Tuch, T., Velarde, F., Quincey, P., Seeger, S., Nowak, A. (2018). Mobility particle size spectrometers: Calibration procedures and measurement uncertainties. Aerosol Sci. Technol. 52, 146–164. https://doi.org/10.1080/02786826.2017.1387229

World Health Organization (WHO) (2021). WHO global air quality guidelines: particulate matter ($PM_{2.5}$ and $PM_{10}$), ozone, nitrogen dioxide, sulfur dioxide and carbon monoxide. World Health Organization. https://iris.who.int/handle/10665/345329

Wu, H., Reis, S., Lin, C., Beverland, I.J., Heal, M.R. (2015). Identifying drivers for the intra-urban spatial variability of airborne particulate matter components and their interrelationships. Atmos. Environ. 112, 306–316. https://doi.org/10.1016/j.atmosenv.2015.04.059

Xiao, S., Wang, M.Y., Yao, L., Kulmala, M., Zhou, B., Yang, X., Chen, J.M., Wang, D.F., Fu, Q.Y., Worsnop, D.R., Wang, L. (2015). Strong atmospheric new particle formation in winter in urban Shanghai, China. Atmos. Chem. Phys. 15, 1769–1781. https://doi.org/10.5194/acp-15-1769-2015

Yang, L., Pandithurai, G., Chate, D.M., Rao, P.S.P., Waghmare, V., Iyer, U. (2019). Evidence of precedent wind role on controlling $PM_1$ wet scavenging of aerosols during monsoon rain events. Atmos. Environ. 201, 265–277. https://doi.org/10.1016/j.atmosenv.2018.12.041

Zhang, Q., Jimenez, J.L., Canagaratna, M.R., Allan, J.D., Coe, H., Ulbrich, I., Alfarra, M.R., Takami, A., Middlebrook, A.M., Sun, Y.L., Dzepina, K., Dunlea, E., Docherty, K., DeCarlo, P.F., Salcedo, D., Onasch, T., Jayne, J.T., Miyoshi, T., Shimono, A., Hatakeyama, S., *et al.* (2007). Ubiquity and dominance of oxygenated species in organic aerosols in anthropogenically-influenced Northern Hemisphere midlatitudes. Geophys. Res. Lett. 34, L13801. https://doi.org/10.1029/2007GL029979